

---

# CytoGAN: Generative Modeling of Cell Images

---

Anonymous Author(s)

Affiliation

Address

email

## Abstract

We explore the application of Generative Adversarial Networks to the domain of morphological profiling of human cultured cells imaged by fluorescence microscopy. When evaluated for their ability to group cell images responding to treatment by chemicals of known classes, we find that adversarially learned representations are superior to autoencoder-based approaches. While currently inferior to classical computer vision and transfer learning, the adversarial framework enables useful visualization of the variation of cellular images due to their generative capabilities.

## 1 Introduction

Advances in high-throughput microscopy systems have enabled acquisition of large volumes of high-resolution cell images [3]. This paves the way for novel computational methods that can leverage these large quantities of data to study biological systems. Our work focuses on the task of morphological profiling, which aims to map microscopy images of cells to representation vectors that capture salient features and axes of variation in an unsupervised manner [4]. These representations ideally divide the morphological space into clusters of cells with similar properties or, in the case of induced perturbations, similar function.

Current techniques for morphological profiling broadly fall in two categories: a) classical image processing, using specialized software like CellProfiler [5] to capture representations via manually-tuned segmentation and traditional computer vision pipelines, and b) transfer learning to extract features learned by deep convolutional neural networks originally trained to classify miscellaneous objects [16, 1]. Classical computer vision approaches offer better interpretability of features but require more human tuning of the segmentation algorithms, and are limited by the feature set implemented in the image analysis software. Current transfer learning techniques have been shown to outperform classical methods in at least one dataset [16, 1]. However, given that these networks were trained on natural images (in RGB), they do not discover the relations of the biologically meaningful image channels. Instead, their superior performance is likely due to their ability to extract high-level vision features, which appear to capture the overall structure of cells, but not necessarily all the intricate details of their morphological variations. Therefore, we hypothesized that learning representations specifically adapted to cell images would be valuable.

We employ Generative Adversarial Networks (GANs) [7] to build a generative model of single cell images from the BBBC021 dataset [12]. We show that this model learns rich feature representations and synthesizes realistic images that are useful for exploring morphological variation in cells. The main advantages of this method are:

- *Adaptability*: Unsupervised representation learning, which can readily incorporate new data. This is important given that applications of morphological profiling usually lack ground truth annotations, but instead aim to reveal the structure of the image collection.

- *Specialization*: Because this method learns from its training data it is able to disentangle factors of variation and extract inherent semantic relationships. Transfer learning approaches lack this ability and cannot capture the intrinsic relations between the biologically meaningful channels.
- *Translating into biological phenotypes*: The generative abilities of this model enable useful visualizations of cells to help translate data variations into meaningful biological phenotypes.

## 2 Related Work

Our work lies at the intersection of automated morphological profiling, and representation learning with deep neural networks, in particular generative architectures. Caicedo et al. [3] recently outlined the state and challenges of the morphological profiling problem. Prior to this, Ljosa et al. [11] compared the performance of various dimensionality reduction techniques for CellProfiler features on the BBBC021 benchmark [12], consisting of MCF7 cells exposed to different chemical treatments. Pawlowski et al. [16] for the first time reported a representation-learning method based on deep learning that is competitive with hand-engineered features at the task of predicting mechanism-of-action (MOA) of chemicals. Ando et al. [1] also applied transfer learning with a different architecture and introduced a novel feature normalization method. Other related work on this dataset include supervised classification [10], transfer learning on CellProfiler features [9], and dimensionality reduction using autoencoders [19].

Few published studies have applied unsupervised deep learning techniques to the task of feature extraction in morphological profiling. Pawlowski [15] first investigated autoencoder-based methods but reported results far inferior to hand-tuned features or transfer-learning approaches. Our model is more related to the work by Osokin et al. [14] and Johnson et al. [8], wherein GANs were used to model cell images, although their applications did not include morphological profiling.

## 3 Using GANs for Representation Learning

Goodfellow et al. [7] introduced GANs as a game of two players: a *generator*  $G$  and a *discriminator* or *critic*  $D$ . The former receives samples  $\mathbf{z}$  drawn from a noise prior  $P_{\text{noise}}$  which it maps to values  $G(\mathbf{z})$  that should resemble elements of some data distribution  $P_{\text{data}}$ . The discriminator must learn to distinguish such synthetic samples from real values  $\mathbf{x} \sim P_{\text{data}}$ . The critic’s confidence in the realism of the generator’s productions is used as feedback to  $G$ , guiding it to synthesize ever more realistic replicates of samples from the data prior. This procedure is formalized in a zero-sum game,

$$\min_G \max_D V(G, D) = \mathbb{E}_{\mathbf{x} \sim P_{\text{data}}} [\log(D(\mathbf{x}))] + \mathbb{E}_{\mathbf{z} \sim P_{\text{noise}}} [\log(1 - D(G(\mathbf{z})))].$$

Radford et al. [17] first specialized GANs to image synthesis by introducing Deep Convolutional GANs (DCGANs). DCGANs implement the generator and discriminator based on convolutional operations. Derivations of DCGANs such as Least Squares GAN (LSGAN) [13] or Wasserstein GAN (WGAN) [2] tackle instabilities in the training procedure of early generative adversarial models. In our experiments, we found LSGAN to be most stable, in part leading to higher quality generated images than both DCGAN and WGAN.

The original GAN framework does not include an explicit means of performing inference. As such, we require extensions that allow mapping of a sample  $\mathbf{x}$  drawn from the data prior to a latent representation via some encoder transformation  $E(\mathbf{x})$ . A common approach is to interpret the penultimate layer of the discriminator as a latent space. The activations of this layer serve as a source of representation vectors. These latent codes are thought to be meaningful because the discriminator must develop a strong internal representation of its input to succeed at its discrimination task. Furthermore, this method imposes no computational overhead compared to vanilla GANs. More advanced encoders could tie this encoding to a corresponding noise vector.

## 4 Exploring Biological Phenotypes Using Cell Image Synthesis

GANs have been proven to synthesize realistic images both within and beyond the biological domain [7, 17, 14]. We examine if this ability transfers to cell images extracted from the BBBC021 dataset of

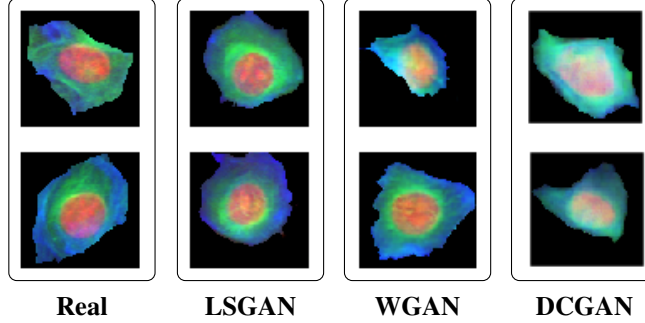


Figure 1: Examples of real BBBC021 cell images juxtaposed with synthetic cell images generated with LSGAN, WGAN and DCGAN. LSGAN synthesizes the most realistic images as judged by our expert biologists.

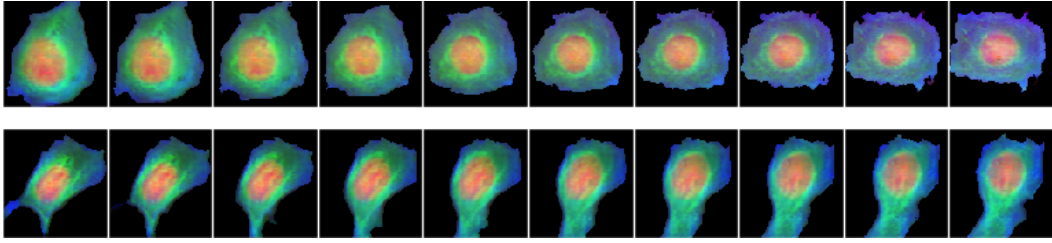


Figure 2: Interpolating between two points  $\mathbf{z}_1, \mathbf{z}_2 \sim P_{\text{noise}}$  results in smooth transitions in the synthesized cell images. Each row shows the transition from  $\mathbf{z}_1$  to  $\mathbf{z}_2$  from left to right.

78 human breast cancer cell lines. Each image in BBBC021 consists of three *channels* corresponding to  
 79 DNA, F-Actin and  $\beta$ -Tubulin, cellular components visualized by fluorescence microscopy. We stack  
 80 these channels and treat them as RGB images via a simple  $\text{DNA} \mapsto \text{R}, \beta\text{-Tubulin} \mapsto \text{G}, \text{F-Actin} \mapsto \text{B}$   
 81 mapping. We obtain ca. 1.3 million single cell images by segmenting the raw images using  
 82 CellProfiler. Finally, we normalize the luminance of each channel to the range  $[0 - 1]$ .

83 Figure 1 shows examples of images generated with LSGAN, WGAN and DCGAN architectures  
 84 alongside real images. The synthetic images, particularly those produced by LSGAN, are not only  
 85 highly detailed and realistic, but also consistent with their biological nature. For example, it is  
 86 characteristic that  $\beta$ -Tubulin forms a circular halo cradling the nucleus. This property is maintained  
 87 clearly in all generated images.

88 Current approaches to morphological profiling extract features that are challenging to translate into  
 89 biological meaning, such as Zernike moments. While other features capture readily understandable  
 90 concepts such as the area occupied by the nucleus, even these are difficult to interpret when a given  
 91 class of cells is defined by several such features in combination. For transfer learning it is nearly  
 92 impossible to visualize the concept of a feature. In contrast, the noise space of GANs is known to  
 93 be highly interpretable and reveal rich semantic structure [17]. We are able to demonstrate this for  
 94 images of cells. Figure 2 exhibits how interpolating between two noise samples leads to smooth  
 95 transitions in synthesized cells. This supports the fact that the generator learned a low-dimensional  
 96 manifold of the images. Figure 3 shows that the noise space encodes semantic relationships, enabling  
 97 algebra on interpretable properties of the images such as size of the nucleus or  $\beta$ -Tubulin content.  
 98 While there is no way to encode images into  $P_{\text{noise}}$  with the methods presented so far, we believe more  
 99 advanced architectures that enable this will be highly valuable if they can maintain these remarkable  
 100 semantic properties.

## 101 5 Representation Learning for Morphological Profiling

102 We test the quality of representations extracted via the discriminator by evaluating their ability to  
 103 cluster treatments of similar function, here the mechanism-of-action. We obtain treatment profiles by

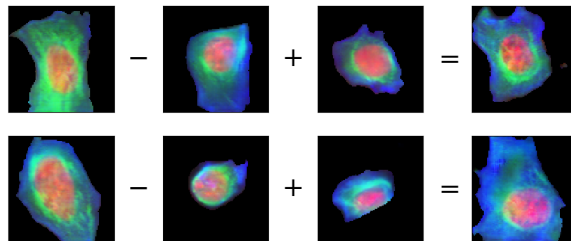


Figure 3: Vector algebra in the noise space translates to biologically valuable relationships in generated images. In the first row, subtracting the vector for a cell with small quantities of  $\beta$ -Tubulin (green stain) from one with high amounts yields a vector representation for "higher  $\beta$ -Tubulin content". In the second row, the difference between a large and small nucleus encodes the semantic meaning of "larger nucleus", which can be added to vectors of other cell images to grow the size of the nucleus.

DCGAN	WGAN	LSGAN	VAE [15]	CP [18]	Deep Transfer [16]	Deep Transfer [1]
43 %	45 %	63 %	49 %	90 %	91 %	96 %

Table 1: Comparison of the mechanism-of-action classification accuracy. CP refers to the results by Singh et al. [18] using CellProfiler features. The Deep Transfer methods correspond to Deep Feature Transfer as proposed by Pawlowski et al. [16] and refined by Ando et al. [1].

104 averaging the extracted single cell representations found as intermediate activations of the discrimina-  
 105 tor. Further, we follow the experimental protocol of [11] and report an average MOA classification  
 106 accuracy of a leave-one-compound-out cross-validation using a one nearest neighbor classifier.

107 Table 1 compares the accuracy of our technique to classical CellProfiler features and transfer learning.  
 108 We found that the quality of representations extracted by our approach is not yet competitive with other  
 109 methods. Nevertheless, we believe that the adversarial approach has significant benefits regarding  
 110 its ability to translate into biological phenotypes as outlined above. Additionally, this framework is  
 111 able to adapt to the dataset at hand and extract inherent relations that are not captured by previous  
 112 techniques. We believe that further improvements are possible, as the quality of synthesized images  
 113 correlates with classification accuracy. Accordingly, the best performing method (LSGAN) also  
 114 yields the highest image quality, as judged qualitatively by expert biologists and shown in Figure 1.

## 115 6 Conclusion

116 This work investigates the use of GANs for the domain of cell microscopy imaging, in particular mor-  
 117 phological profiling. First, we demonstrate the abilities of our generative model with the exploration  
 118 of morphological phenotypes by synthesizing realistic images of cells and performing transforma-  
 119 tions on them such as interpolation and vector algebra. Second, we extend standard GANs with an  
 120 encoder and assess the quality of learned representations by evaluating their mechanism-of-action  
 121 classification performance following [11]. Even though adversarially learned representations are  
 122 currently inferior at this task, we argue that further enhancements to GANs and encoding schemes  
 123 will lead to biologically richer latent representations and better MOA classification accuracy.

124 This work covers only a small fraction of possible applications of GANs to the domain of microscopy  
 125 images. For example, we hope that future work investigates BiGANs[6] or other novel solutions to  
 126 infer latent features with GANs. We believe that improved inference, combined with the interpretable  
 127 nature of the GAN framework, may enable simulated experiments by performing algebra with vectors  
 128 corresponding to cell lines, diseases or other perturbations. Finally, we note that deep learning  
 129 generally flourishes with larger amounts of data. Thus, we conjecture that the performance of the  
 130 outlined approaches will improve with larger datasets.

## References

- [1] D Michael Ando, Cory McLean, and Marc Berndl. Improving phenotypic measurements in high-content imaging screens. *bioRxiv*, page 161422, 2017.
- [2] Martin Arjovsky, Soumith Chintala, and Léon Bottou. Wasserstein gan. *arXiv preprint arXiv:1701.07875*, 2017.
- [3] Juan C Caicedo, Sam Cooper, Florian Heigwer, Scott Warchal, Peng Qiu, Csaba Molnar, Aliaksei S Vasilevich, Joseph D Barry, Harmanjit Singh Bansal, Oren Kraus, et al. Data-analysis strategies for image-based cell profiling. *Nature methods*, 2017.
- [4] Juan C Caicedo, Shantanu Singh, and Anne E Carpenter. Applications in image-based profiling of perturbations. *Current Opinion in Biotechnology*, 39:134–142, 2016.
- [5] Anne E Carpenter, Thouis R Jones, Michael R Lamprecht, Colin Clarke, In Han Kang, Ola Friman, David a Guertin, Joo Han Chang, Robert a Lindquist, Jason Moffat, Polina Golland, and David M Sabatini. CellProfiler: image analysis software for identifying and quantifying cell phenotypes. *Genome biology*, 7(10):R100, 2006.
- [6] Jeff Donahue, Philipp Krähenbühl, and Trevor Darrell. Adversarial feature learning. *arXiv preprint arXiv:1605.09782*, 2016.
- [7] Ian Goodfellow, Jean Pouget-Abadie, Mehdi Mirza, Bing Xu, David Warde-Farley, Sherjil Ozair, Aaron Courville, and Yoshua Bengio. Generative adversarial nets. In *Advances in neural information processing systems*, pages 2672–2680, 2014.
- [8] Gregory R Johnson, Rory M Donovan-Maiye, and Mary M Maleckar. Generative modeling with conditional autoencoders: Building an integrated cell. *arXiv preprint arXiv:1705.00092*, 2017.
- [9] C. Kandaswamy, L. M. Silva, L. A. Alexandre, and J. M. Santos. High-Content Analysis of Breast Cancer Using Single-Cell Deep Transfer Learning. *Journal of Biomolecular Screening*, 2016.
- [10] Oren Z. Kraus, Jimmy Lei Ba, and Brendan J. Frey. Classifying and segmenting microscopy images with deep multiple instance learning. *Bioinformatics*, 32(12):i52–i59, 2016.
- [11] V. Ljosa, P. D. Caie, R. ter Horst, K. L. Sokolnicki, E. L. Jenkins, S. Daya, M. E. Roberts, T. R. Jones, S. Singh, A. Genovesio, P. A. Clemons, N. O. Carragher, and A. E. Carpenter. Comparison of Methods for Image-Based Profiling of Cellular Morphological Responses to Small-Molecule Treatment. *Journal of Biomolecular Screening*, 18(10):1321–1329, 2013.
- [12] Vebjorn Ljosa, Katherine L Sokolnicki, and Anne E Carpenter. Annotated high-throughput microscopy image sets for validation. *Nature Methods*, 9(7):637–637, 2012.
- [13] Xudong Mao, Qing Li, Haoran Xie, Raymond YK Lau, Zhen Wang, and Stephen Paul Smolley. Least squares generative adversarial networks. *arXiv preprint ArXiv:1611.04076*, 2016.
- [14] Anton Osokin, Anatole Chessel, Rafael E Carazo Salas, and Federico Vaggi. Gans for biological image synthesis. *arXiv preprint arXiv:1708.04692*, 2017.
- [15] Nick Pawlowski. Towards Image-Based Morphological Profiling using Deep Learning Techniques. Master’s thesis, University of Edinburgh, 2016.
- [16] Nick Pawlowski, Juan C Caicedo, Shantanu Singh, Anne E Carpenter, and Amos Storkey. Automating morphological profiling with generic deep convolutional networks. *NIPS 2016 Workshop on Machine Learning in Computational Biology*, 2016.
- [17] Alec Radford, Luke Metz, and Soumith Chintala. Unsupervised representation learning with deep convolutional generative adversarial networks. *arXiv preprint arXiv:1511.06434*, 2015.
- [18] S. Singh, M. A. Bray, T. R. Jones, and A. E. Carpenter. Pipeline for illumination correction of images for high-throughput microscopy. *Journal of Microscopy*, 256(3):231–236, 2014.
- [19] Lee Zamparo and Zhaolei Zhang. Deep Autoencoders for Dimensionality Reduction of High-Content Screening Data. *arXiv preprint arXiv:1501.01348*, 2015.